Analysis of Pressure Gradient Across Aortic Stenosis with Massively Parallel Computational Simulations

Amanda Randles[1,2], Erik Draeger[1], Franziska Michor[2]

[1]Lawrence Livermore National Laboratory, Livermore, CA, USA
[2]Dana-Farber Cancer Institute, Boston, MA,USA

Abstract

Coarctation of the aorta (CoA) is one of the most common congenital heart defects in the United States, and despite treatment, patients have a decrease in life expectancy. Computational fluid dynamics simulations can provide the physician with a non-invasive method to measure the pressure gradient. With HARVEY, a massively parallel hemodynamics application, patient specific simulations can be conducted of large regions of the vasculature. The pressure across the stenosis is impacted by flow from nearby vessels. The purpose of this study was to study the impact of including these distal vessels in the simulation on the resulting pressure measurements. Computational fluid dynamic simulations were conducted in three subsets of one patient's vasculature. We demonstrate up to a 29% difference in calculated pressure gradient based on the number of vessels included in the simulation. These initial results are positive but need to be substantiated with further patient studies.

1. Introduction

Coarctation of the aorta (CoA) is characterized by a severe narrowing of the aorta that can lead to congestive heart failure. It accounts for 5-8% of congenital heart defects in the United States each year [1]. Current clinical practice is to take a course of action that reduces the pressure gradient across the narrowing, or stenosis, to below 20 mmHg as a high gradient can result in an increased cardiac workload [2]. Treatment options such as surgical repair, balloon angioplasty, and stent implantation have proven successful in the short term; however, long term results reveal decrease in life expectancy and predilection for hypertension, early onset coronary disease, stroke and aneurysm formation [3].

Image-based computational fluid dynamics (CFD) have started to be widely used to study the localization and progression of vascular diseases, such as atherosclerosis and aneurysms [4, 5]. Recent efforts have targeted the development of models that capture the impact of stress conditions on patients presenting CoA [6]. Most research has focused on prognostic and diagnostic methods and there is little work studying the impact of the size of the circulatory region included in the simulation. There is a need for an analysis of key macroscopic risk factors and the impact of including flow from distal vessels.

By developing a highly efficient computational tool for image-based flow simulation, studies of large regions of the circulatory system can now be studied at high resolutions. In this paper, we present a method for obtaining pressure measurements in patient-based models. We compare the results for three different subsections of one patient's vasculature. Unlike previous studies that either model simply the region around a stenosis or focus on the large network of vessels, our approach focuses on the pressure gradient across the identical coarctation while including a range of extra vessels. We demonstrate up to a 29% difference in calculated pressure gradient based on the number of vessels included in the simulation. The remainder of this paper illustrates the impact that large-scale parallel simulations can have even when assessing the risk factors across small distinct regions of the human vasculature.

2. Methods

Conventional medical imaging modalities like CT or MRI scans are used to acquire medical imaging data which are then segmented to create a triangular mesh representing the geometry of the vessels. A computational grid is initialized to describe the volume enclosed by this mesh and serve as input to the CFD algorithm. The mesh can also be anatomically edited to enable virtual surgery before flow simulation. A feedback loop is in place to optimize the outcome and guide treatment planning.

The geometry used in this paper is from de-identified pre-existing imaging studies provided as part of the Vascular Model Repository [7]. The geometry of the vessels was obtained through gadolinium-enhanced MR angiography (MRA) with a 1.5-T GE Signa scanner. A segmented

mesh file was created using customized SimVascular software (Simtk.org). Flow rates were measured by PC-MRI sequence encoding and provided for the duration of a cardiac cycle [8].

2.1. Patient-Specific Computational Fluid Modeling

To enable personalized simulations of blood flow in the aorta, we have developed a massively parallel computational hemodynamics application, HARVEY, based on the lattice Boltzmann method (LBM). The LBM is an alternative to the traditional Navier-Stokes equation for modeling fluid flow. The volume of a 3-dimensional mesh is filled with a regular array of lattice points on which a minimal form of the classical Boltzmann equation is simultaneously solved for a set of fictitious particles. We use an embedded boundary method to convert the triangular mesh of the vessel geometry to the regular Cartesian grid needed for the LBM simulation. We create an axis-aligned bounding box of the mesh and discretize its volume into a grid of the necessary resolution. As the vascular geometries are typically non-convex, we base our property testing on Bærentzen and Aanæs' angle weighted pseudo normal approach [9] that allows us to classify grid points as fluid, inlet, outlet, wall, or exterior nodes using the pseudo normal at the corresponding closest point on the vessel manifold [10].

To obtain 3-dimensional flow information we apply the LBM to the aortic domain calculated and prescribe personalized inflow and outflow boundary conditions. The LBM is a low-Mach, weakly compressible solver that can efficiently model flow through complex geometries such as the human vasculature [11], [12]. At the tradeoff of small time steps and use of a high-resolution grid, such explicit finite difference schemes lend themselves to highly efficient parallel implementations.

The fundamental quantity is the particle distribution function, denoted $f_i(\vec{x}, t)$, representing the likelihood that a particle is at grid point x, at time t, and traveling with discrete velocity ξ. The fluid dynamics are resolved through the evolution of $f_i(\vec{x}, t)$ with time:

$$f(\vec{x}+\xi_i\Delta t, t+\Delta t) = f(\vec{x}, t) - \omega\Delta t(f(\vec{x}, t) - f^{eq}(\vec{x}, t)). \quad (1)$$

There are two key components of the algorithm: advection and collision. In the advection portion of each time step, the particles are propagated along the velocity paths defined by the lattice discretization. Fluid-fluid collisions are then handled through a relaxation towards a local equilibrium, shown on the right side of Eq. 1. We leverage the Bhatnager-Gross-Krook (BGK) operator, a collision operator that relaxes to equilibrium on a single time scale. The
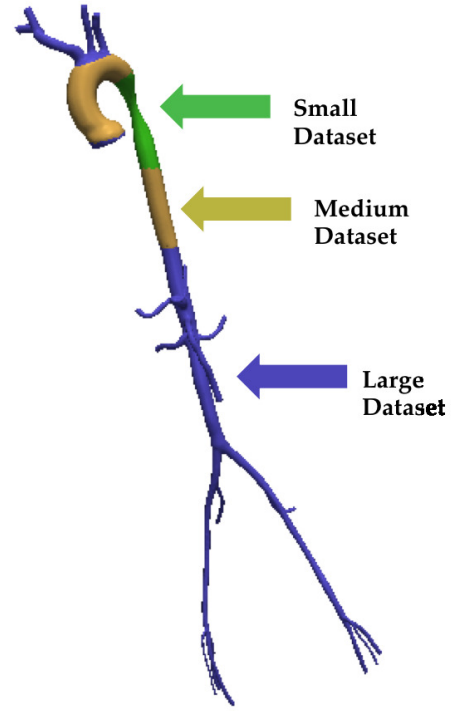

Figure 1. **Dataset Definitions.** The three dataset sizes used in these studies are defined. The green region highlights a small dataset containing only the stenosis. The gold region depicts the medium dataset containing a large portion of the aorta and the purple region shows the large dataset including a large section of the aorta femoral vasculature.

relaxation frequency ω is related to the kinematic viscosity of the fluid $\nu = c_s^2\Delta t(\frac{1}{\omega} - \frac{1}{2})$. The equilibrium distribution is defined with density ρ and speed u as:

$$f_i^{eq} = w_i\rho\left[1 + \frac{\vec{c}_i \cdot \vec{u}}{c_s^2} + \frac{1}{2}\left(\frac{(\vec{c}_i \cdot \vec{u})^2}{(c_s^2)^2} - \frac{u^2}{c_s^2}\right)\right] \quad (2)$$

where w denotes the quadrature weight normalized to unity and the speed of sound is a lattice constant: $c_s^2 = \frac{1}{3}$.

Another advantage of the LBM is that macroscopic quantities such as density are moments of the distribution function. This means that they can be calculated based on its summation and therefore are available entirely locally. Pressure is calculated locally through the ideal gas relation: $P = c_s^2\rho$.

3. Small Case Study

To study the impact of the vasculature region included in the simulation on the resulting pressure gradient across

the coarctation, we selected one patient arterial geometry as shown in Fig. 1.

This geometry was then separated into three distinct data sets: (1) small dataset representing the conventional model of including only the stenosed region (green) (2) medium dataset including the full aortic arch (gold) (3) large dataset including a large portion of the aortofemoral vasculature (purple). We use Blender software (open source shareware, www.blender.org), a modeling and animation application, to modify the triangular mesh and enforce a closed mesh after vessel extraction. We chose Blender because it is free and compatible with our mesh representations, but we expect most mesh editing and CAD software to be sufficient for the task of anatomical editing. Each dataset presents an increasingly computationally expensive problem. In this paper, we used a 10 micron resolution grid as bulk-fluid simulations have been shown to demonstrate convergence with (at most) this resolution [13]. The resulting grid sizes are shown in Table 1.

Table 1. Number of Fluid Nodes Per Dataset.

Small	821,242
Medium	652,331
Large	198,887

In order to model the flow in the largest set, we used 16,384 processors of the IBM Blue Gene/Q supercomputer; taking advantage of the parallel optimizations described in [14]. A Newtonian behavior of the blood was assumed with a density of 0.001 gr/mm^3 and a dynamic viscosity of 0.004 gr/mm/sec. The Zou-He boundary conditions were implemented in which a patient-specific inflow velocity was prescribed at the inlet and a constant pressure gradient was applied out the outlets. The inflow velocity was obtained via a 2D, phase-contrast (PC) MRI sequence with through-plane velocity encoding [8].

4.   Results

Detailed pressure distribution maps were generated for each of the three datasets. The result for the large set is shown in Fig. 2.

The risk factor of interest in this study as the pressure gradient across the coarctation. The blue lines depict the planes across which this factor was measured. The average and maximal pressure gradients for each dataset were measured and are shown in Fig. 2. The effect of accounting for larger regions of the vasculature is highlight in Fig. 3, showing a greater than 29% increase in calculated pressure gradient for the small dataset as compared to the large dataset. The change in both the mean and maximal pres-
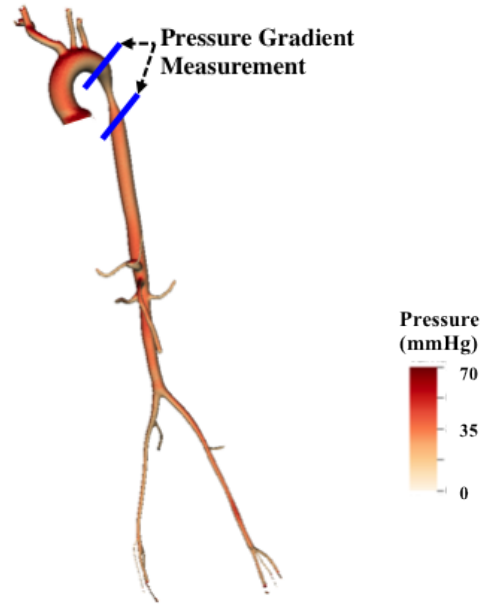

Figure 2. **Pressure Map.** The pressure profile map is shown from the large dataset simulation. Regions of high pressure are shown in red. The slices from which the pressure gradient is calculated are indicated by the blue lines.

sure gradient between the medium and large datasets were both approximately 3%. These results highlight the fact that the pressure is not only dependent on the severity of the coarctation but also the flow profile and geometry of the vasculature feeding into the stenosis. It is therefore necessary to simulate the hemodynamic outcome rather than simply measuring the degree of narrowing to determine the severity of the coarctation.

5.   Conclusion

We have presented here a tool for patient-specific assessment of risk factors associated with cardiovascular disease. Through a case study of one patient with a severe CoA, we investigated the impact of including large regions of the vasculature. The pressure metrics showed that the flow coming from distal vessels can have a dramatic impact on the pressure gradient across a stenosis, making it necessary to include them in image-based simulations. Such models increase the computational intensity of the problem and require large-scale models for accurate modeling. Further studies including a larger patient cohort and spanning a range of physiological conditions are needed to further quantify the regions required for accurate modeling.
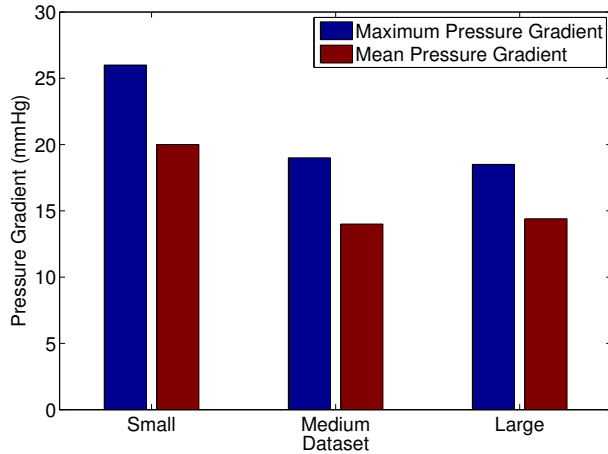
Figure 3. **Pressure Gradient.** The mean and maximal pressure gradient measured across the stenosis is shown for each dataset.

Acknowledgements

References

[1] Love BA, Fischer GW, Stelzer P, Fuster V. Aortic coarctation in the adult. Pediatric and Congenital Cardiology Cardiac Surgery and Intensive Care 2014;2521–2549.

[2] Ralovich K, Itu L, Mihalef V, Sharma P, et al. Hemodynamic assessment of pre-and post-operative aortic coarctation from mri. In Medical Image Computing and Computer-Assisted Intervention–MICCAI 2012. Springer, 2012; 486–493.

[3] Magee A, Brzezinska-Rajszys G, Qureshi S, et al. Stent implantation for aortic coarctation and recoarctation. Heart 1999;82(5):600–606.

[4] Grinberg L, Morozov V, Fedosov D, et al. A new computational paradigm in multiscale simulations: Application to brain blood flow. In High Performance Computing, Networking, Storage and Analysis (SC), 2011 International Conference for. IEEE, 2011; 1–12.

[5] Peters A, Melchionna S, et al. Multiscale simulation of cardiovascular flows on the ibm bluegene/p: Full heart-circulation system at red-blood cell resolution. In Proceedings of the 2010 ACM/IEEE International Conference for High Performance Computing, Networking, Storage and Analysis. 2010; 1–10.

[6] Karmonik C, Brown A, Debus K, Bismuth J, Lumsden AB. CFD challenge: Predicting patient-specific hemodynamics at rest and stress through an aortic coarctation. In Statistical Atlases and Computational Models of the Heart. Imaging and Modelling Challenges. Springer, 2014; 94–101.

[7] Wilson NM, et al. The vascular model repository: A public resource of medical imaging data and blood flow simulation results. Journal of Medical Devices 2013;7(4):040923.

[8] Ladisa JF, et al. Computational simulations for aortic coarctation: representative results from a sampling of patients. Journal of Biomechanical Engineering 2011; 133(9):091008.

[9] Bærentzen JA, Anaæs H. Signed distance computation using the angle weighted pseudonormal. IEEE Transactions on Visualization and Computer Graphics May 2005; 11(3):243–253.

[10] Peters Randles A, Bächer M, Pfister H, Kaxiras E. A lattice boltzmann simulation of hemodynamics in a patient-specific aortic coarctation model. In Statistical Atlases and Computational Models of the Heart. Imaging and Modelling Challenges. Springer, 2013; 17–25.

[11] Chen S, Doolen G. Lattice boltzmann method for fluid flows. Annual review of fluid mechanics 1998;30(1):329–364.

[12] Succi S. The lattice Boltzmann equation: for fluid dynamics and beyond. Oxford university press, 2001.

[13] Peters A, Melchionna S, Kaxiras E, Lätt J, Sircar J, Bernaschi M, Bison M, Succi S. Multiscale simulation of cardiovascular flows on the IBM Blue Gene/P: Full heart-circulation system at red-blood cell resolution. In Proceedings of the 2010 ACM/IEEE International Conference for High Performance Computing, Networking, Storage and Analysis, SC '10. IEEE Computer Society. ISBN 978-1-4244-7559-9, 2010; .

[14] Peters Randles A, Kale V, J.R. Hammond, Gropp W, Kaxiras E. Performance analysis of the lattice Boltzmann model beyond Navier-Stokes. In Proceedings of the 27th IEEE International Parallel and Distributed Processing Symposium, IPDPS '13. 2013; .

Address for correspondence:

Amanda Randles
7000 East Ave. Livermore, CA 94550
randles2@llnl.gov